Long-term X-ray Spectral Variability Study of the Quasar PDS 456

Fida Fathima S S
Presidency University, Kolkata

Collaborators:
Tathagata Saha (IUCAA, Pune)
Arijit Sar (Presidency University, Kolkata)
Ritaban Chatterjee (Presidency University, Kolkata)

The Young Astronomers Meeting 2026
18 – 20 March, 2026

Contents

Active Galactic Nuclei (AGN)

- Compact size (<< 1 pc)
- Powered by accretion onto the SMBH
- Very high luminosity ($\sim 10^{42}$ - 10^{48} erg.s^{-1})
- Emits enormous energy across the electromagnetic spectrum
- AGN show high X-ray variability from hours to decades

PDS 456

- Nearby radio-quiet Quasar (z=0.184)
- Most luminous quasar in the local universe ($L_{bol} \sim 10^{47} ergs^{-1}$)
- Black hole mass ~ $10^9 M_\odot$
- Ultra-fast outflow (UFO) with velocities between 0.25-0.3c
- Rapid X-ray variability

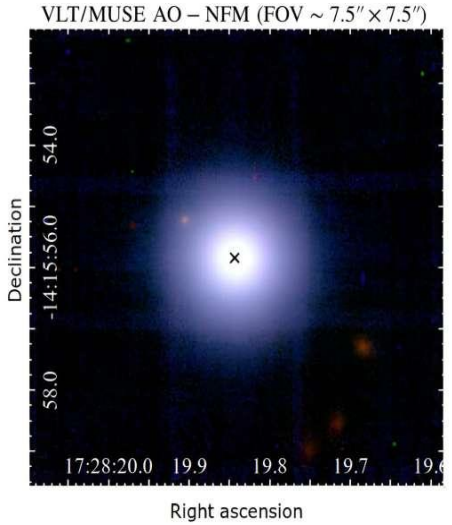

Credit: Travascio et al. 2024.

AstroSat

- India's First Multi-wavelength Space Observatory
- Launched by ISRO in 2015
- Provides simultaneous multi-wavelength coverage from UV to hard X-rays.
- Enables broadband spectral & timing studies of compact objects and transients

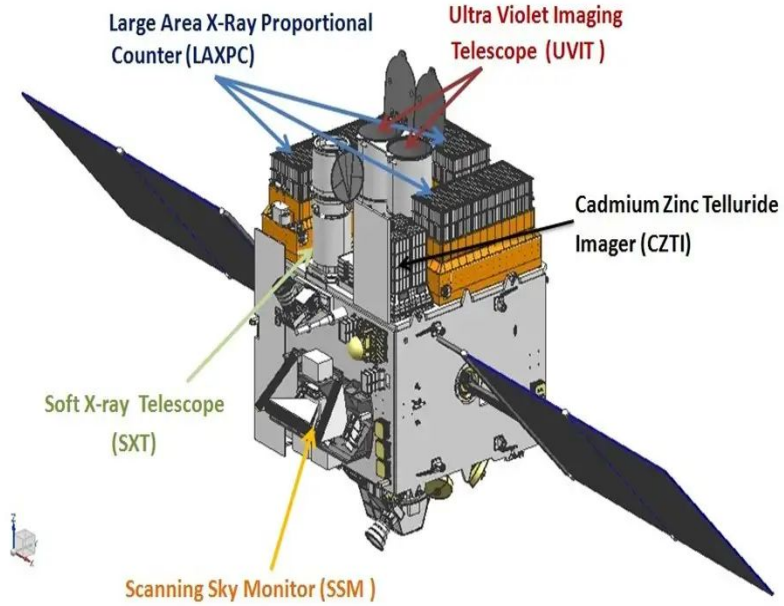

AstroSat Observations

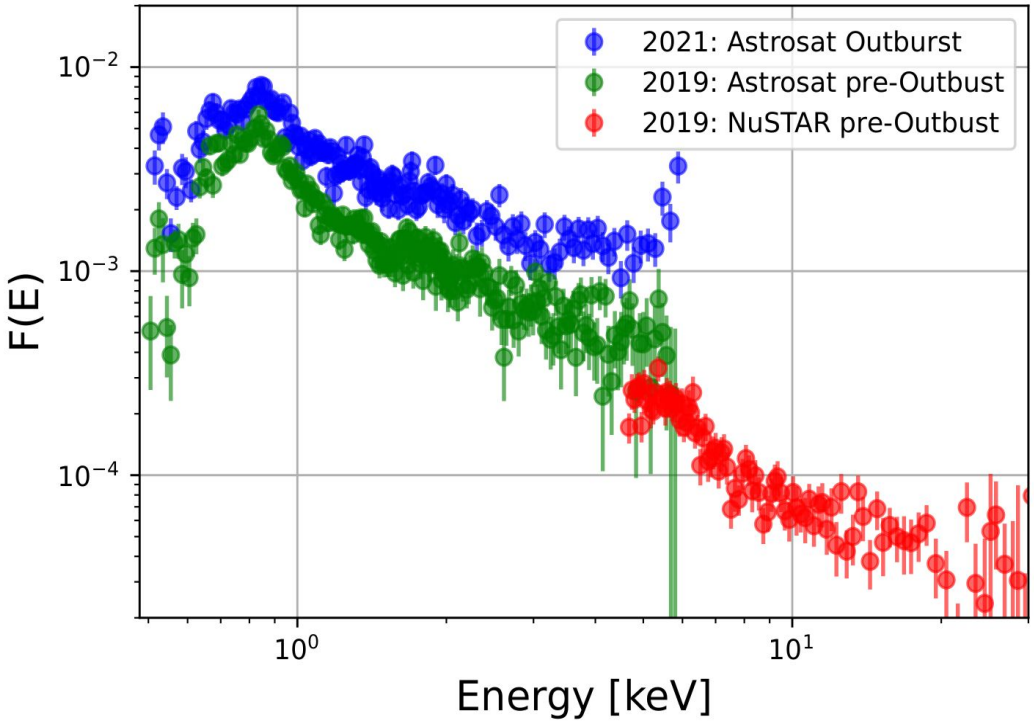

Following the flaring episode in 2018, AstroSat observed the source in a low-flux state in 2019, followed by re-brightening in 2021

Long-term X-ray Spectral Variability Study of PDS 456

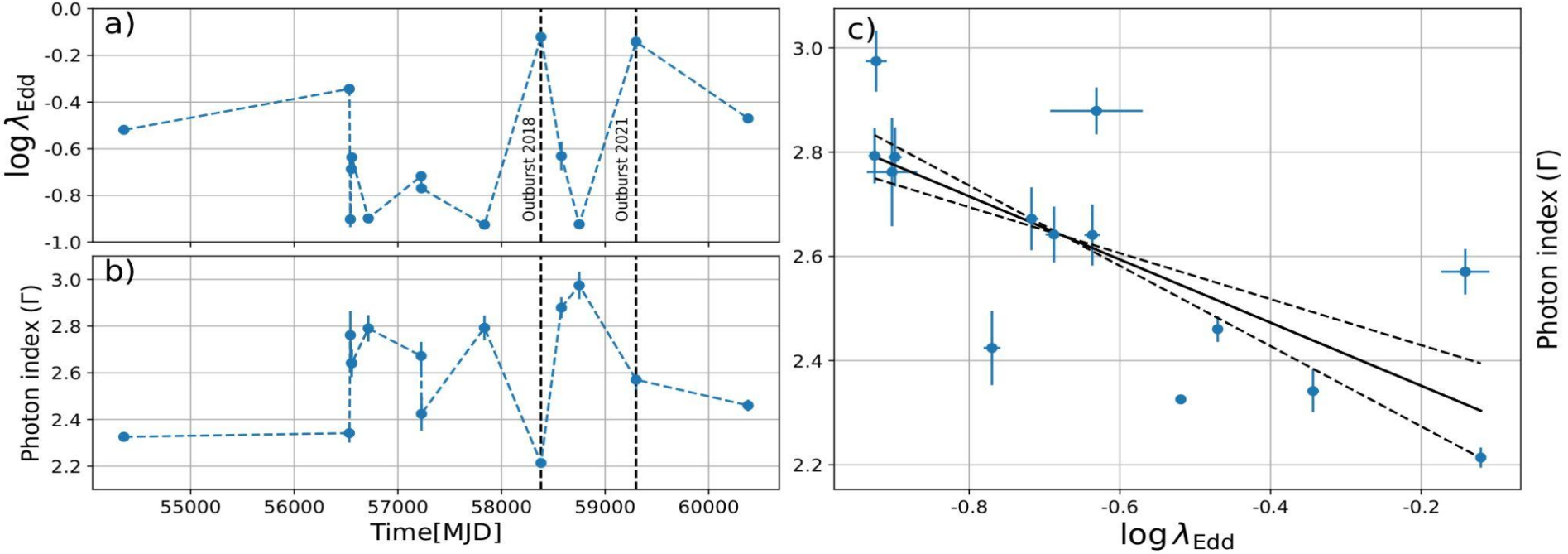

(a) A drastic increase in the Eddington ratio is seen 2018 and 2021.

(b) In the high-flux state, the photon index remains consistently lower.

(c) Softer when fainter trend is observed.

★ K_{bol} is taken from Duras et al. 2020

reXcor

- Self-consistently combines ionized relativistic reflection and warm-corona emission.
- Accretion energy in the inner disc is distributed between: warm corona, hot lamppost X-ray source, accretion disc
- Simultaneous fitting of relativistic reflection and the soft excess

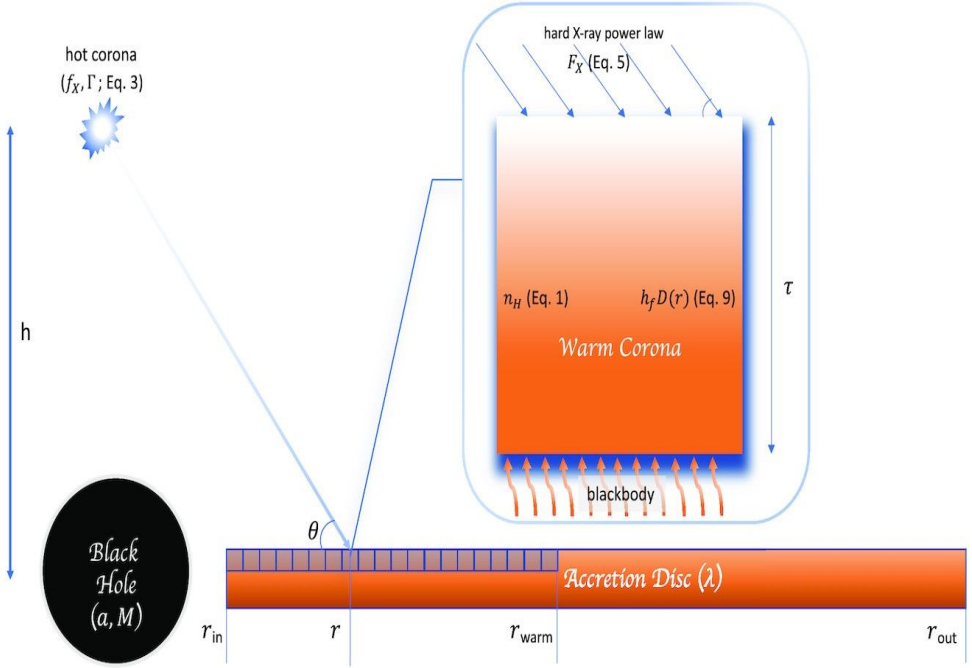

Xiang et al. 2022

XMM-Newton + NuSTAR (2013)

Model: constant × tbabs (cutoffpl + reXcor)

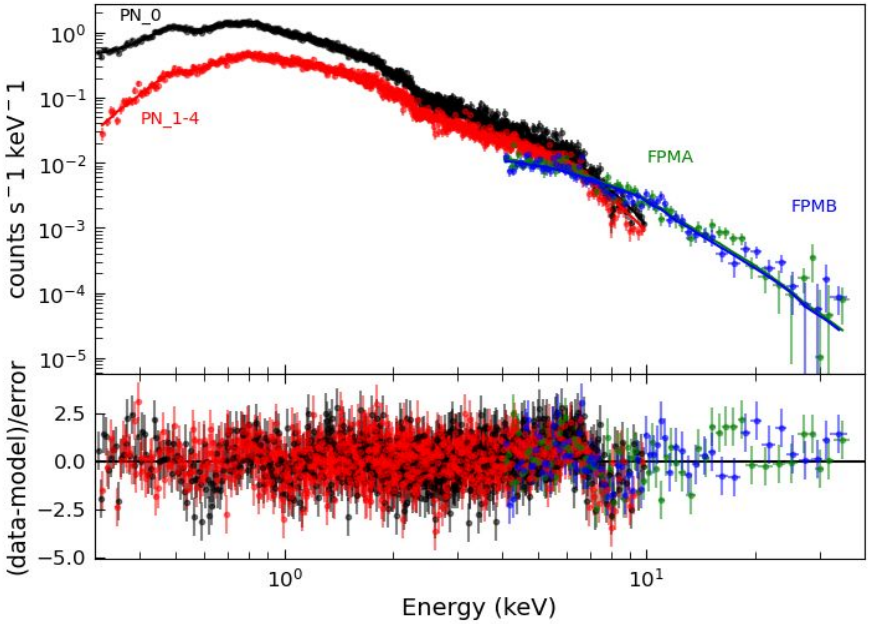

reXcor (l=0.1,a=0.99,h=5)

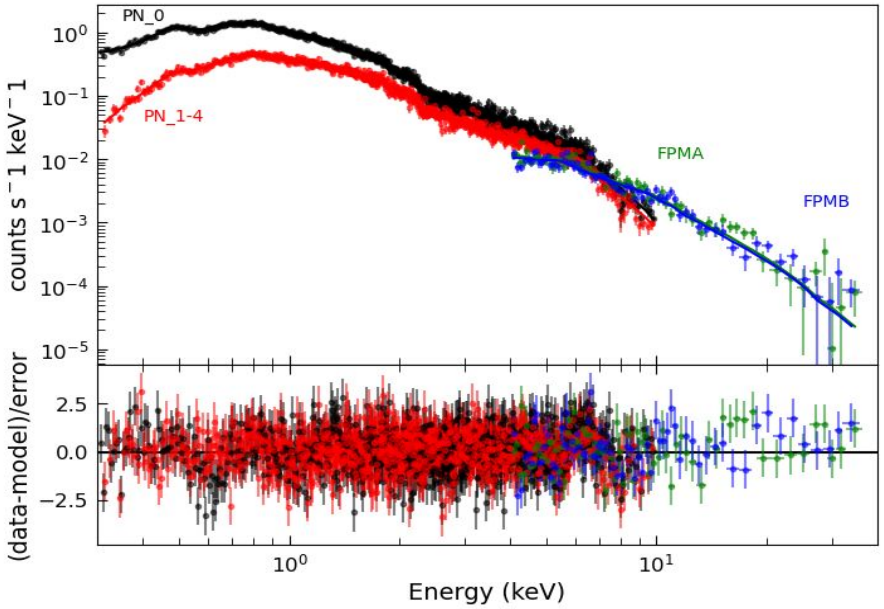

reXcor (l=0.1,a=0.99,h=20)

Parameters	**reXcor (l=0.1,a=0.99,h=5)**	**reXcor (l=0.1,a=0.99,h=20)**
Γ	$2.33^{+0.02}_{-0.06}$	2.30 +/- 0.05
High_Ecut (keV) cutoffpl	> 43.1	$25.4^{+24}_{-9.3}$
Lamppost heating fraction (f_x)	$0.04^{+0.02}_{-0.01}$	$0.13^{+0.03}_{-0.02}$
Warm corona heating fraction (h_f)	$00.12^{+0.05}_{-0.01}$	< 0.03
τ	<11.7	$10.6^{+0.44}_{-0.38}$
$\frac{\chi^2}{\mathrm{dof}}$	1908.95/1725	1817.81/1725

XMM-Newton + NuSTAR (2018)

Model: constant × tbabs (cutoffpl + reXcor)

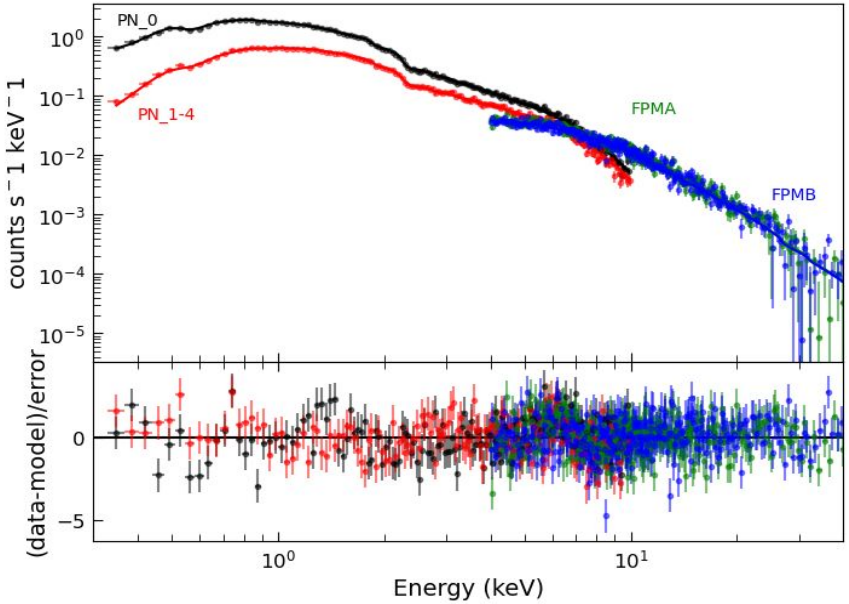

reXcor (l=0.1,a=0.99,h=5)

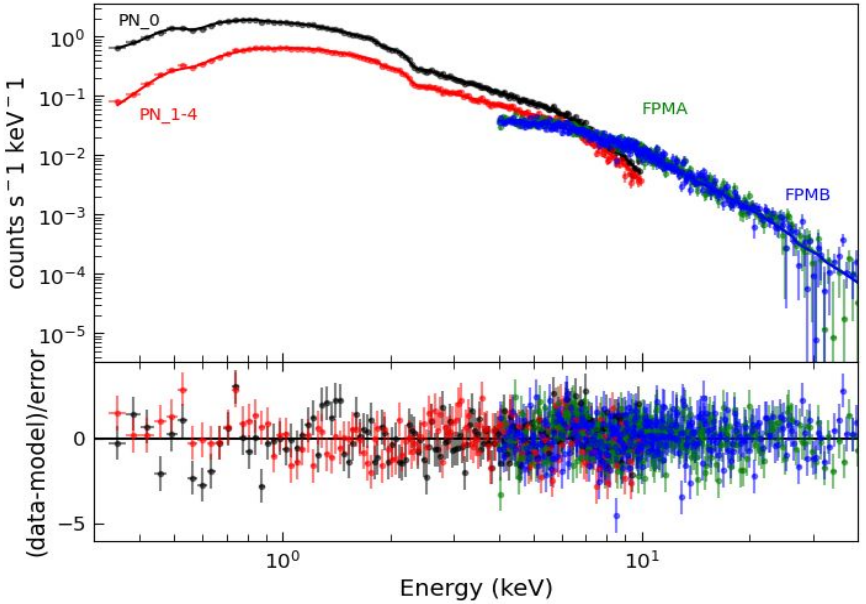

reXcor (l=0.1,a=0.99,h=20)

Parameters	**reXcor (l=0.1,a=0.99,h=5)**	**reXcor (l=0.1,a=0.99,h=20)**
Γ	1.97 +/- 0.02	1.96 +/- 0.02
High_Ecut (keV) cutoffpl	$50.7^{+15.1}_{-9.43}$	$34.1^{+7.28}_{-5.27}$
Lamppost heating fraction (f_x)	$0.03^{+0.03}_{-0.01}$	> 0.05
Warm corona heating fraction (h_f)	$0.12^{+0.05}_{-0.02}$	$0.51^{+0.06}_{-0.25}$
τ	$11.4^{+1.21}_{-0.71}$	> 18.8
$\frac{\chi^2}{\text{dof}}$	1121.10/930	1083.43/930

AstroSat Observation (2021)

Model: tbabs (zpowerlaw + reXcor)

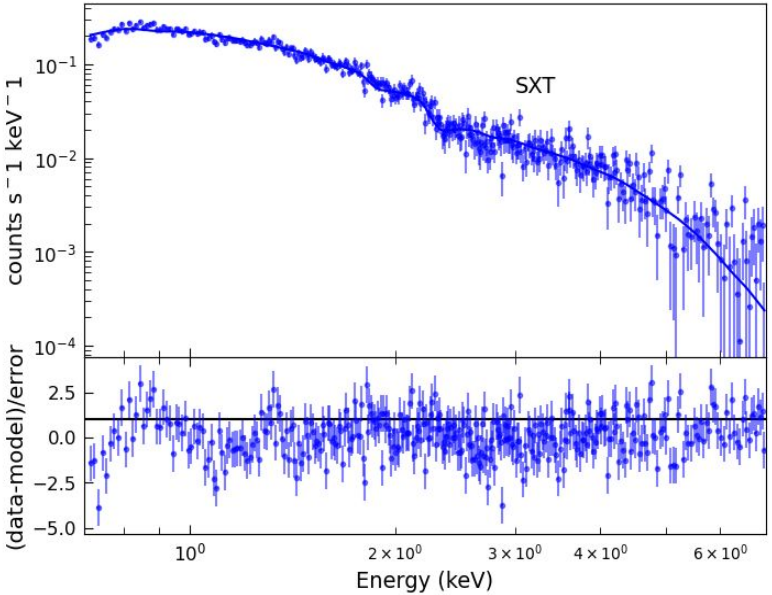

reXcor (l=0.1,a=0.99,h=5)

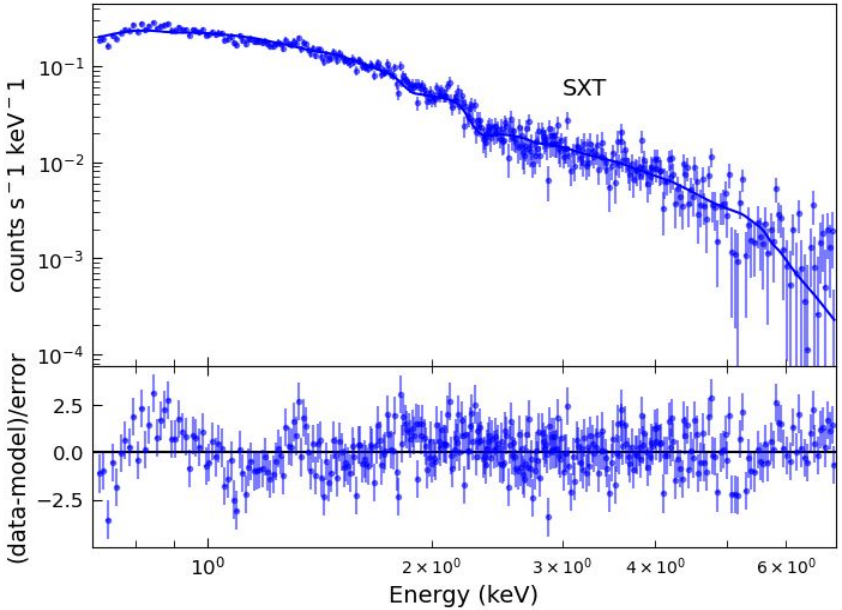

reXcor (l=0.1,a=0.99,h=20)

Parameters	**reXcor (l=0.1,a=0.99,h=5)**	**reXcor (l=0.1,a=0.99,h=20)**
Γ	2.17 +/- 0.06	2.09 +/- 0.07
Lamppost heating fraction (f_x)	$0.14^{+0.01}_{-0.03}$	< 0.04
Warm corona heating fraction (h_f)	<0.015	$0.65^{+0.03}_{-0.04}$
τ	<10.03	>23.32
$\frac{\chi^2}{\mathrm{dof}}$	434.87/351	467.02/351

Fe Kα Flux vs Continuum Flux

- tbabs(zpowerlw + zgauss)
- A positive correlation is observed at low–intermediate flux states
- At the highest flux levels, the Fe line shows a weaker response to the continuum, coinciding with the transition to warm-corona dominated spectra.

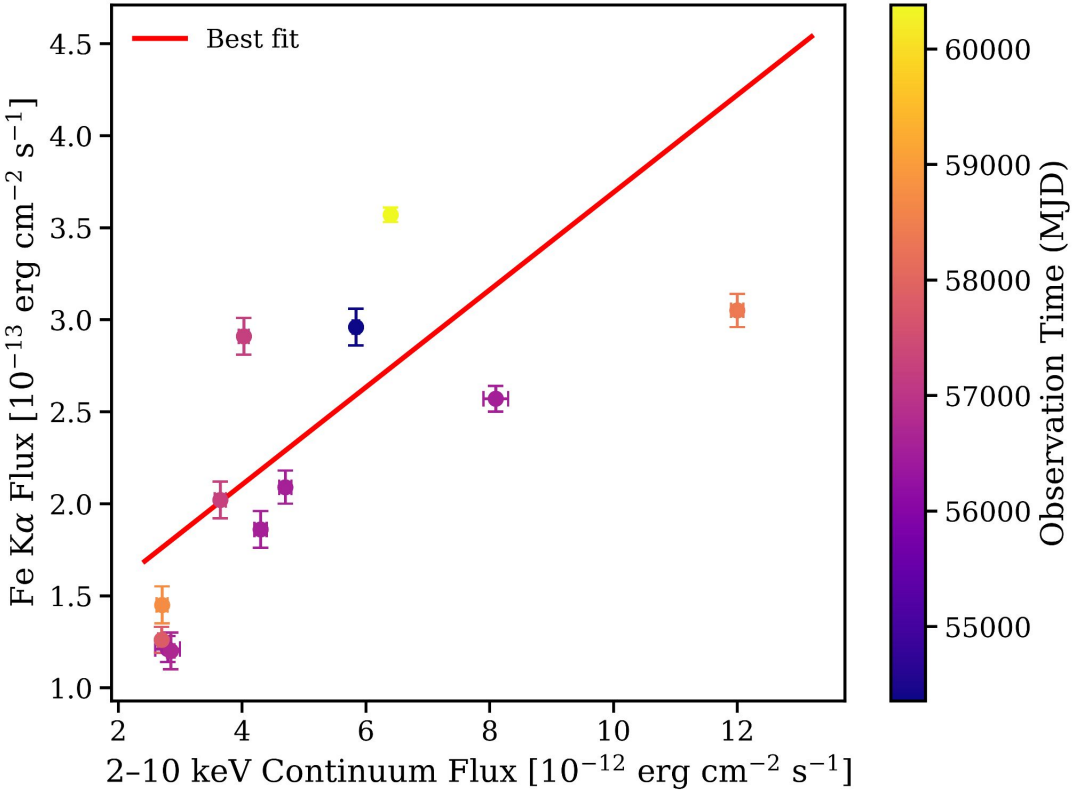

Results

- The spectrum becomes harder as the flux increases
- The accretion flow could be advection dominated
- Our result is consistent with Reeves et al. (2021), who reported a high-energy cutoff of ~50 keV.
- At 20 Rg, the low-flux state is reflection-dominated, while both flaring states show strong warm-corona dominance.
- The disk–corona energy balance appears flux-dependent, with reflection not changing proportionally when the warm corona becomes dominant.

THANK YOU

Time	Obs. Id.	Telescope	Abbreviation	Obs. mode	GTI Exp. [a] (ks)	Counts[b]	Comm.	optical/UV
2007-09-12	0501580101	*XMM-Newton*	XMM1	FW	69.3	2.40×10^5	–	UVM2
2013-08-27	60002032002	*NuSTAR*	Nu1	–	43.8	1.18×10^4	–	–
2013-09-06	60002032004	*NuSTAR*	Nu2	–	42.9	2.98×10^3	–	–
2013-09-15	60002032006	*NuSTAR*	Nu3	–	44.0	6.98×10^3	–	–
2013-09-20	60002032008	*NuSTAR*	Nu4	–	58.5	8.94×10^3	–	–
2014-02-26	60002032010	*NuSTAR*	Nu5	–	109.3	9.8×10^3	–	–
2015-07-21	90101008002	*NuSTAR*	Nu6	–	40.8	1.1×10^4	–	–
2015-07-24	90101008004	*NuSTAR*	Nu7	–	77.2	5.8×10^3	–	–
2017-03-23	60201020002	*NuSTAR*	Nu8	–	158.0	2.2×10^4	–	–
2018-09-20	60402007002	*NuSTAR*	Nu9	–	81.9	3.4×10^4	–	–
2019-09-24	60402007004	*NuSTAR*	Nu10	–	78.3	7.2×10^3	–	–
2019-04-11	A05_046T01_9000002834	*Astrosat*	As1	–	245	5.1×10^4	–	–
2021-03-26	A10_007T01_9000004276	*Astrosat*	As2	–	67.1	2.3×10^4	–	–
2021-04-30	A10_007T01_9000004350	*Astrosat*	As3	–	120.0	4.1×10^4	–	–
2024-03-10	60901011002	*NuSTAR*	Nu11	–	159.2	3.3×10^4	–	–

Time (MJD)	Flux(4–10 keV) 10^{-12} erg cm^{-2} s^{-1}	Flux(2–10 keV) 10^{-12} erg cm^{-2} s^{-1}	$\log \lambda_{\rm Edd}$	Γ
54355.1	3.13±0.03	5.84±0.05	-0.520±0.004	2.33±0.01
56531.2	4.31±0.08	8.1±0.2	-0.34±0.01	2.34±0.04
56541.1	1.51±0.12	2.8±0.2	-0.90±0.03	2.8±0.1
56550.7	2.29±0.06	4.3±0.1	-0.69±0.01	2.64±0.05
56555.1	2.52±0.06	4.7±0.1	-0.64±0.01	2.64±0.06
56714.3	1.53±0.03	2.85±0.06	-0.90±0.01	2.79±0.06
57224.5	2.16±0.04	4.03±0.08	-0.72±0.01	2.67±0.06
57227.5	1.96±0.05	3.65±0.09	-0.77±0.01	2.42±0.07
57835.2	1.45±0.03	2.70±0.05	-0.93±0.01	2.79±0.05
58381.1	6.42±0.06	12.0±0.1	-0.120±0.004	2.21±0.02
58578.0	2.54±0.36	4.7±0.7	-0.63±0.06	2.97±0.09
58750.4	1.45±0.05	2.71±0.09	-0.92±0.01	2.88±0.06
59299.0	6.19±0.46	11.6±0.9	-0.14±0.03	2.57±0.04
60379.9	3.43±0.04	6.40±0.07	-0.47±0.01	2.46±0.02

MCMC Corner plot for AstroSat/SXT 2021 obs.